Journal of Organometallic Chemistry 751 (2014) 604–609

Contents lists available at ScienceDirect

Journal of Organometallic Chemistry

journal homepage: www.elsevier.com/locate/jorganchem

Synthesis, structural characterization and cytotoxicity of bimetallic chlorogold(I) phosphine complexes employing functionalized phosphinoferrocene carboxamides

Jiří Schulz [a], Jiří Tauchman [a], Ivana Císařová [a], Tina Riedel [b], Paul J. Dyson [b], Petr Štěpnička [a,*]

[a] Department of Inorganic Chemistry, Faculty of Science, Charles University in Prague, Hlavova 2030, CZ-12840 Prague, Czech Republic
[b] Institute of Chemical Sciences and Engineering, Ecole Polytechnique Fédérale de Lausanne (EPFL), CH-1015, Lausanne, Switzerland

ARTICLE INFO

Article history:
Received 12 June 2013
Received in revised form
27 June 2013
Accepted 5 July 2013

Keywords:
Bioorganometallic chemistry
Gold complexes
Phosphine ligands
Ferrocene ligands
Anticancer activity
X-ray crystallography

ABSTRACT

Gold(I) phosphine complexes of the general formula [AuCl($Ph_2PfcCONHY$-κ*P*)], where Y is CH_2CO_2Me (**7**), CH_2CONH_2 (**8**), CH_2CH_2OH (**9**), $CH(CH_2OH)_2$ (**10**), $C(CH_2OH)_3$ (**11**), and $CH_2SO_3(HNEt_3)$ (**12**), and fc is ferrocene-1,1′-diyl, were prepared from [AuCl(tht)] (tht = tetrahydrothiophene) and the appropriate phosphinoferrocene carboxamides (**1**–**6**). The compounds were characterized by spectroscopic and analytical methods, and the molecular structures of **7** and **9** were determined by single-crystal X-ray crystallography. Complexes **7**–**12** exerted antiproliferative activity against the human ovarian cancer cells *in vitro*. The IC_{50} values ranged ca. 0.3–3.7 μM for the A2780 cell line, and 3.1–20 μM for the cisplatin resistant cell line A2780R, with complex **7** being the most cytotoxic against both cell types. IC_{50} values for the non-tumorigenic human embryonic kidney (HEK) cells, serving as a measure of a general toxicity, were found in roughly similar ranges, i.e. 0.9–6.8 μM.

1. Introduction

Amide linkage represents a chemically and structurally well-defined way to conjugate diverse molecular moieties. Not surprisingly, therefore, amide linkers have been widely used in the design of functional phosphine donors that display useful catalytic and biological properties [1]. During our studies on phosphinoferrocene carboxamides prepared from 1′-(diphenylphosphino)ferrocene-1-carboxylic acid (Hdpf) [2] and polar functional amines (Scheme 1) such as aminosulfonic acids [3], amino acid esters [4,5] and hydroxyamines [6,7], we reasoned that the attached functional pendants can affect bioavailability of transition metal complexes prepared from such phosphinoamide ligands (a bulky lipophilic complex with a hydrophilic tag) or alternatively act as a directing group. Indeed, transition metal–phosphine complexes have been widely explored in medicinal chemistry [8] and a gold–phosphine complex (auranofin) is used in the clinic to treat arthritis [9]. Auranofin also displays significant cytotoxicity toward a range of different cancer cells [10], and a large number of gold(I) phosphine complexes exhibit potent cytotoxic activity *in vitro* and antitumor activity *in vivo* [11].

Moreover, there is considerable interest in the biological activity and medicinal properties of ferrocene-based compounds [12] with simple ferrocene compounds exhibiting good cytotoxicities *in vitro* and tumor growth inhibition *in vivo* [13]. Jaouen has shown that appending the ferrocenyl group to biologically active molecules affords complexes with an increased potency with tumor specificity possibly due to the combined action of the organic molecule with Fenton chemistry of the iron centre [14]. There are also numerous reports describing the cytotoxic effects of bimetallic, ferrocene-containing compounds including platinum [15],

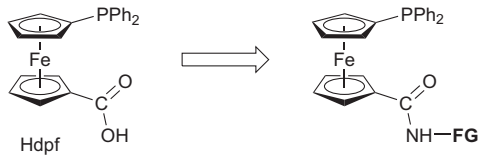

Scheme 1. Design of functional phosphinoferrocene carboxamides. **FG** stands for a functional moiety.

* Corresponding author. Fax: +420 221 951 253.
E-mail address: stepnic@natur.cuni.cz (P. Štěpnička).

0022-328X/$ – see front matter © 2013 Elsevier B.V. All rights reserved.
http://dx.doi.org/10.1016/j.jorganchem.2013.07.014

palladium [16], ruthenium [9] and gold(I) [11] phosphinoferrocene complexes. The association of two active metals showed cytotoxic activities comparable or superior to cisplatin in various cancer cell lines.

We recently evaluated the cytotoxic properties of Pd(II) and Pt(II) complexes bearing a phosphinoferrocene carboxamide possessing 2-hydroxyethyl substituent at the amide nitrogen as P-monodentate donor [16] and of (η^6-arene)Ru(II) complexes with phosphinoferrocene amides derived from amino acid esters [17]. This contribution extends our work toward gold(I) complexes and phosphinoferrocene carboxamides derived from amino acid esters, aminosulfonates and hydroxyamines.

2. Results and discussion

2.1. Synthesis of the Au(I) complexes 7–12

The neutral gold(I) complexes **7**–**12** were prepared in a straightforward manner by the substitution of the labile tetrahydrothiophene (tht) ligand in the precursor complex [AuCl(tht)] with the stoichiometric amount of the appropriate phosphinoferrocene carboxamide **1**–**6** (Scheme 2). The complexes were isolated in good yields as air-stable, somewhat light sensitive solids that were characterized by NMR and IR spectroscopy, electrospray ionization (ESI) mass spectrometry and elemental analysis.

The ^{1}H NMR spectra of **7**–**12** corroborate the anticipated structures, as do the ^{31}P NMR spectra, which display resonances in a narrow range, δ_P 28.5–28.7, downfield with respect to the free ligands. The IR spectra of the complexes show the characteristic bands due to the amide moieties, i.e. the NH stretching vibrations and, mainly, the strong amide I and amide II bands at 1625–1650 cm^{-1} and around 1530 cm^{-1}, respectively.

2.2. Molecular structure of complexes 7 and 9

The molecular structure of **7** is shown in Fig. 1 and the selected bond parameters are summarized in Table 1. Compound **9** crystallizes with two molecules per the asymmetric unit. A view of molecule 1 is shown in Fig. 2 with key bond parameters for both structurally independent molecules given in Table 2. As indicated by the overlap (Fig. 2), the independent molecules of **9** differ mainly by the conformation of their polar amide pendants, which seems to reflect the different roles the molecules have to play in the solid-state assembly (see below).

The geometry of the fcPPh$_2$–Au–Cl moieties (fc = ferrocene-1,1′-diyl) in **7** and both crystallographically independent molecules

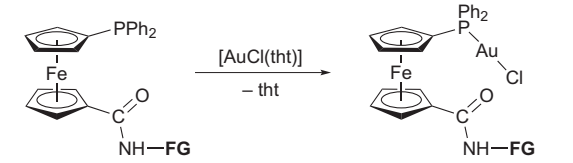

FG = CH_2CO_2Me (**1**)
CH_2CONH_2 (**2**)
CH_2CH_2OH (**3**)
$CH(CH_2OH)_2$ (**4**)
$C(CH_2OH)_3$ (**5**)
$CH_2SO_3(HNEt_3)$ (**6**)

FG = CH_2CO_2Me (**7**)
CH_2CONH_2 (**8**)
CH_2CH_2OH (**9**)
$CH(CH_2OH)_2$ (**10**)
$C(CH_2OH)_3$ (**11**)
$CH_2SO_3(HNEt_3)$ (**12**)

Scheme 2. Preparation of Au(I) complexes **7**–**12**. **FG** denotes a functional group, tht is tetrahydrothiophene.

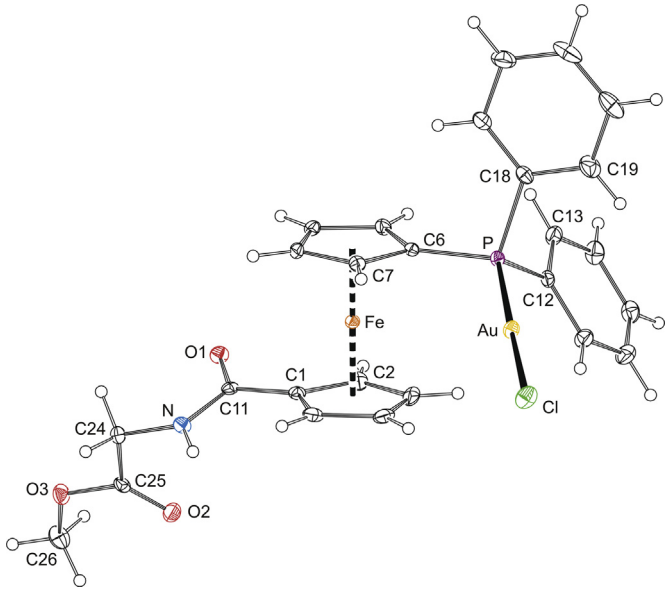

Fig. 1. PLATON plot of the molecular structure of **7** showing the atom labeling scheme and displacement ellipsoids at the 30% probability level.

of **9** are similar to each other and also compare well to those reported previously for, e.g., $(Et_2NH_2)[ClAuPh_2PfcCO_2]$ [18], $[ClAuPh_2PfcEPh]$ (E = S and Se) [19], $[ClAuPh_2PfcCH_2NMe_2]$ and $[ClAuPh_2PfcCH_2NHMe_2]X$ (X = Cl and ClO_4) [20], and for complexes of the type $[ClAuPh_2PfcY]$, where Y is 2- or 3-pyridyl, and CH_2(2-pyridyl) [21]. Likewise, the geometric parameters describing the amide pendant do not digress significantly from those reported for uncoordinated amides **1** and **3** and their palladium complexes [4,6]. The ferrocene units in both structurally independent molecules possess regular geometries, showing only marginal variations in the individual Fe–C distances (Fe–C: 2.022(2)–2.054(2) Å for **7**; 2.035(5)–2.061(4) Å for **9**, molecule 1, and 2.025(5)–2.056(4) Å for **9**, molecule 2) and, accordingly, an insignificant tilting (**7**: 1.6(1)°, **9**: ca. 3.5°). The ferrocene cyclopentadienyl rings in **7** adopt an intermediate conformation with τ = −164.9(2)° that brings the substituents in positions 1 and 1′ of the ferrocene unit into mutually opposite positions. On the other hand, the substituents in both molecules of **9** assume synclinal eclipsed conformations (cf. the τ angle in Table 2 with the ideal value of 72°).

In the solid state, the molecules of **7** associate into infinite chains via C=O···H–N hydrogen bonds around the crystallographic 2_1 screw axes (Fig. 3). In contrast, the molecules of **9** form dimers constituted from molecules 1 and 2 via pairs of N–H···Cl

Table 1
Selected distances and angles for **7** (Å and deg).[a]

Distances		Angles	
Au–Cl	2.2976(6)	Cl–Au–P	176.91(2)
Au–P	2.2396(6)	$\angle Cp^P,Cp^C$	1.6(1)
Fe–Cg^P	1.643(1)	T	−164.9(2)
Fe–Cg^C	1.653(1)	N–C11–O1	122.5(2)
C11–O1	1.230(2)	C11–N–C24	120.9(2)
C11–N	1.350(3)	O2–C25–O3	124.6(2)
C25–O2	1.196(3)	C11–N–C24–C25	74.9(2)
C25–O3	1.339(3)	N–C24–C25–O2	−0.7(3)

[a] Definitions: Cp^P and Cp^C denote the PPh$_2$- and amide-substituted cyclopentadienyl rings, respectively. Cg^P and Cg^C stand for the respective ring centroids. τ = C1–Cg^C–Cg^P–C6.

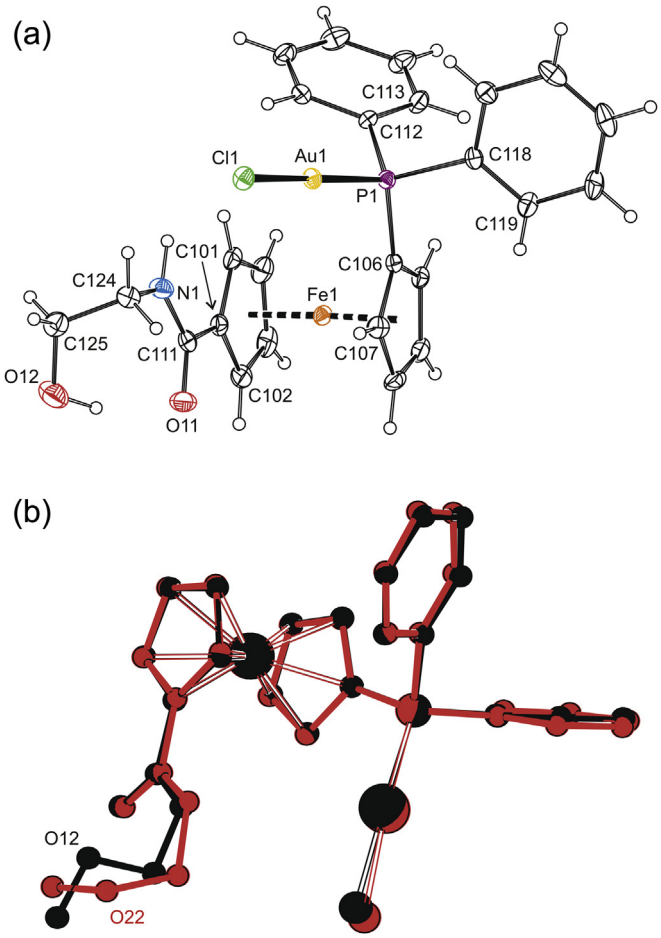

Fig. 2. (a) PLATON plot of molecule 1 in the structure of **9** showing the atom labeling scheme and displacement ellipsoids at the 30% probability level. Note: the respective atomic labels in molecule 2 are obtained by changing the first digit to two. (b) Overlap of the two structurally independent molecules (molecule 1 in black, molecule 2 in red). (For interpretation of the references to colour in this figure legend, the reader is referred to the web version of this article.)

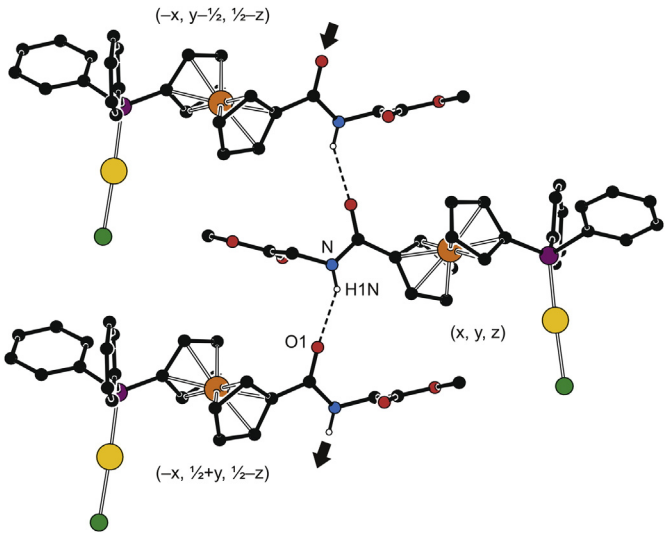

Fig. 3. Section of the infinite hydrogen-bonded chain in the structure of **7**. For clarity, all CH hydrogens were omitted. The H-bond parameters are as follows: N···H1N···O1^{i}, N1···O1^{i} = 2.875(2) Å, angle at H1N = 150°; i. (–*x*, ½+*y*, ½–*z*).

hydrogen bonds (Fig. 4). These dimers further assemble into infinite ribbons through O22–H2O···O12 interactions while the other OH group (O12–H1O in molecule 1) forms an intramolecular hydrogen bridge toward the amide oxygen O11. No significant Au···Au (aurophilic) contacts were observed in both structures [22].

2.3. Cytotoxicity tests

The antiproliferative activity of **7**–**12** has been studied on the ovarian cancer cell lines A2780 and A2780cisR, the latter having acquired resistance to cisplatin, and on human embryonic kidney cells (HEK), a non-tumorigenic model. IC_{50} values are summarized in Table 3. The complexes display high cytotoxicities, with IC_{50} values in the low micromolar region ranging 0.27–3.7 μM for the A2780 cell line and 0.94–6.8 μM for the HEK cell line.

The most active complexes are **7** and **9** which contain glycine ester and hydroxyethyl substituents, respectively. With IC_{50} values of 0.27 ± 0.01 μM (**7**) and 0.6 ± 0.05 μM (**9**) respectively for the A2780 cell line, and 3.1 ± 0.5 μM (**7**) and 6.5 ± 0.5 μM (**9**) for the

Table 2
Selected distances and angles for the crystallographically independent molecules in the structure of **9** (Å and deg).[a]

Molecule 1		Molecule 2	
Au1–Cl1	2.297(1)	Au2–Cl2	2.297(1)
Au1–P1	2.227(1)	Au2–P2	2.227(1)
Cl1–Au1–P1	174.96(4)	Cl2–Au2–P2	177.96(5)
Fe–Cg^{P}	1.643(2)	Fe–Cg^{P}	1.642(2)
Fe–Cg^{C}	1.659(2)	Fe–Cg^{C}	1.648(3)
∠Cp^{P},Cp^{C}	3.4(3)	∠Cp^{P},Cp^{C}	3.4(3)
T1	−74.7(4)	τ2	−76.8(4)
C111–O11	1.248(6)	C211–O21	1.237(8)
C111–N1	1.335(7)	C211–N2	1.338(8)
N1–C111–O11	121.3(5)	N2–C211–O21	120.1(7)
C125–O12	1.413(7)	C225–O22	1.327(9)
N1–C124–C125–O12	71.3(6)	N2–C224–C225–O22	175.0(5)

[a] Definitions: Cp^{P} and Cp^{C} denote the PPh_2- and amide-substituted cyclopentadienyl rings, respectively. Cg^{P} and Cg^{C} are their respective centroids. τ*n* = C*n*01–Cg^{C}*n*–Cg^{P}*n*–C*n*06 (*n* indicates the molecule).

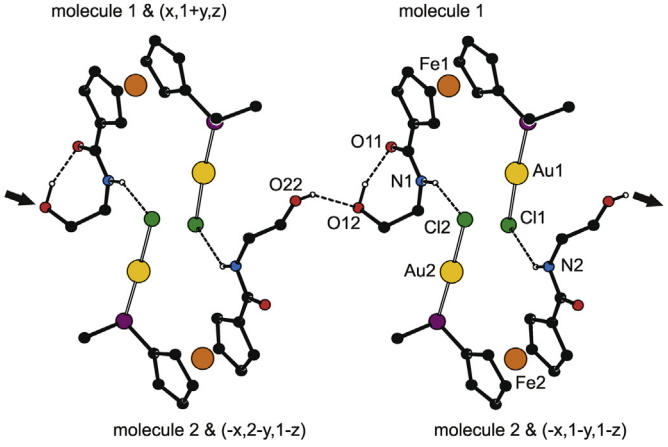

Fig. 4. Depiction of the O–H···O and N–H···Cl interactions in the structure of **9**. For clarity, only the NH and OH hydrogens and the pivotal atoms from the benzene rings are shown. Hydrogen bond parameters are as follows: N1–H1N···Cl2^{i}, N1···Cl2^{i} = 3.324(4) Å, angle at H1N = 147°; N2–H2N···Cl1^{i}, N2···Cl1^{i} = 3.454(4) Å, angle at H2N = 141°; O12–H1O···O11, O12···O11 = 2.748(5) Å, angle at H1O = 159°; O22–H2O···O12^{ii}, O22···O12^{ii} = 2.840(7) Å, angle at H2O = 148°; symmetry codes: i. (–*x*, 1 – *y*, 1 – *z*), ii. (–*x*, 2 – *y*, 1 – *z*).

Table 3
IC_{50} values for A2780 and cisplatin resistant A2780R ovarian cancer cells and for non-tumorigenic HEK cells (exposure: 72 h).

Compound	IC_{50} (A2780) [μM]	IC_{50} (A2780R) [μM]	IC_{50} (HEK) [μM]
7	0.27 ± 0.01	3.1 ± 0.5	0.94 ± 0.07
8	3.7 ± 0.2	20.0 ± 0.1	6.8 ± 0.3
9	0.60 ± 0.05	6.5 ± 0.5	3 ± 1
10	1.5 ± 0.4	10.5 ± 1.3	4.3 ± 0.7
11	1.2 ± 0.3	20.3 ± 0.2	4.6 ± 0.4
12	3.4 ± 0.4	10.6 ± 0.4	5.3 ± 0.3
Cisplatin Ref. [23]	4.3 ± 0.5	18 ± 1	n.a.
Auranofin Ref. [23]	1.3 ± 0.5	1.5 ± 0.3	n.a.

cisplatin resistant cell line, these complexes are more cytotoxic than the reference drug cisplatin [23]. The other compounds exhibit comparable cytotoxicities to cisplatin in A2780 cells as well and marginally lower cytotoxicites in the cisplatin resistant cell line.

The presence of the phosphine–Au–Cl moiety has a strong influence on biological activity. Compared to (η^6-arene)Ru(II) complexes containing the phosphinoferrocene amino acid ester conjugates as P-monodentate donors reported previously [17], replacement of the *p*-cymene ruthenium complex by the Au–Cl moiety leads to a more than 100-fold higher activity. This change is not unexpected as arene ruthenium phosphine complexes tend not to be very cytotoxic [24] and taken together these data indicate that the Au–Cl unit exerts a greater influence on the overall cytotoxicity that the phosphinoferrocene fragment. This is in accordance with our recent study showing that phosphinoferrocene carboxamide bearing a hydroxyethyl substituent (ligand **3**) and palladium(II) and platinum(II) bis(phosphine) complexes derived thereof resulted in negligible cytotoxicity ($IC_{50} > 200$ μM) or IC_{50} values in a moderate micromolar range, respectively [16].

Compounds possessing the highly polar amidoamine and amidosulfonate moieties (**8** and **12**) exert higher IC_{50} values. Finally, exchanging the hydroxyethyl substituent by a bulkier substituent (such as $CH(CH_2OH)_2$ in **10** and $C(CH_2OH)_3$ in **11**) leads to an at least two-fold increase of IC_{50} values for the A2780 and A2780cisR cell lines but not for HEK cells, which might imply that the bulkiness of the substituent plays a significant role in determining the biological activity in cancer cells but not in non-cancerous cells.

3. Conclusions

A series of bimetallic complexes comprising phosphinoferrocene carboxamides coordinated via the phosphine group to AuCl fragment have been prepared and evaluated for their cytotoxicity against human ovarian cancer cells. The particular combination of molecular fragments with different biological activity and physicochemical properties (e.g., solubility and hydrophobicity) results in highly cytotoxic species, with the role of Au–Cl being dominant with respect to the low IC_{50} values (N.B. Our previous study dealing with ligand **3**, the corresponding phosphine oxide and sulfide, and its Pd(II) and Pt(II) complexes revealed that the uncoordinated ferrocene derivatives are practically not cytotoxic [16]). Nevertheless, the two different metal containing units constituting complexes **7**–**12** presumably exert different effects on the cells, e.g., broad acting Fenton chemistry from the ferrocene [14] and, mainly, inhibition of various enzymes by the highly reactive gold(I) unit [25]. Unfortunately, the compounds do not display significant drug selectivity although it may be possible to improve the selectivity by modulating the steric bulk of the substituent at the carboxamide moiety.

4. Experimental

4.1. Materials and methods

All syntheses were performed under argon atmosphere with an exclusion of the direct day light. Compound [AuCl(tht)] [26] and phosphinoferrocene ligands **1**, **2** [4], **3** [6], **4**, **5** [7], and **6** [3] were prepared according to the literature procedures. Anhydrous CH_2Cl_2 (Sigma–Aldrich) and other solvents (Lachner) were used as received.

^{1}H NMR spectra were recorded on a Varian UNITY Inova 400 spectrometer (^{1}H, 399.95 MHz and ^{31}P{^{1}H}, 161.90 MHz) at 298 K. Chemical shifts (δ/ppm) are given relative to internal tetramethylsilane (^{1}H) or to external 85% aqueous H_3PO_4 (^{31}P). ESI-MS were recorded on a Bruker Esquire 3000 spectrometer using samples dissolved in methanol. The formulations of the observed ionic species were confirmed by a comparison of the theoretical and experimentally determined isotopic patterns. Infrared spectra were recorded in Nujol mulls with an FT IR Nicolet Magna 760 instrument.

4.2. Preparation of [AuCl(Ph$_2$PfcCONHCH$_2$CO$_2$Me-κP)] (**7**)

A solution of ligand **1** (97 mg, 0.20 mmol) in dichloromethane (2 mL) was added to solid [AuCl(tht)] (64 mg, 0.20 mmol). The resultant yellow solution was stirred at room temperature for 60 min and filtered into pentane (80 mL). The mixture was allowed to stand overnight at −18 °C before the resulting precipitate was filtered off, washed with cold pentane and dried in vacuo to give **7** as a yellow solid. Yield: 138 mg, 96%. Crystals suitable for X-ray analysis were obtained by slow diffusion of hexane into a toluene solution of **7** at room temperature. ^{1}H NMR ($CDCl_3$): δ 3.75 (s, 3H, OMe), 4.17 (d, $^3J_{HH} = 6.0$ Hz, 2H, NHC*H*$_2$), 4.18 (virtual t, $J \approx 2$ Hz, 2H, fc), 4.49 (virtual q, $J \approx 2$ Hz, 2H, fc), 4.74 (virtual q, $J \approx 2$ Hz, 2H, fc), 4.91 (virtual t, $J \approx 2$ Hz, 2H, fc), 6.59 (t, $^3J_{HH} = 6.0$ Hz, 1H, N*H*CH$_2$), 7.43–7.62 (m, 10H, PPh$_2$). ^{31}P{^{1}H} NMR ($CDCl_3$): δ 28.6 (s). IR (Nujol): ν_{NH} 3360 m, ν_{CO} 1751 vs, amide I 1648 vs, amide II 1533 s cm^{-1}. MS (ESI$^+$): *m*/*z* 756 ([M + K]$^+$), 740 ([M + Na]$^+$), 682 ([M − Cl]$^+$). Anal. Calcd. for $C_{26}H_{24}NO_3PClFeAu$: C 43.51, H 3.37, N 1.95%. Found: C 43.22, H 3.34, N 1.77%.

4.3. Preparation of [AuCl(Ph$_2$PfcCONHCH$_2$CONH$_2$-κP)] (**8**)

Complex **8** was prepared similarly from **2** (94 mg, 0.20 mmol) and [AuCl(tht)] (64 mg, 0.20 mmol) and isolated as a yellow solid. Yield: 133 mg, 92%. ^{1}H NMR ($CDCl_3$): δ 4.08 (d, $^3J_{HH} = 4.2$ Hz, 2H, NHC*H*$_2$), 4.26 (br s, 2H, fc), 4.41 (br s, 2H, fc), 4.70 (br s, 2H, fc), 4.86 (br s, 2H, fc), 6.65, 6.24, 6.85 (3 × br s, 1H, NH), 7.43–7.62 (m, 10H, PPh$_2$). ^{31}P{^{1}H} NMR ($CDCl_3$): δ 28.5 (s). IR (Nujol): ν_{NH} 3338 s, amide I 1683 vs, amide I 1644 vs, amide II 1534 s cm^{-1}. MS (ESI$^+$): *m*/*z* 741 ([M + K]$^+$), 725 ([M + Na]$^+$), 705 ([M − HCl + K]$^+$), 689 ([M − HCl + Na]$^+$), 667 ([M − Cl]$^+$). Anal. Calcd. for $C_{25}H_{23}N_2O_2PClFeAu \cdot 0.3CH_2Cl_2$: C 41.73, H 3.27, N 3.85%. Found: C 41.68, H 3.28, N 3.63%. The content of clathrated solvent was verified by ^{1}H NMR spectroscopy.

4.4. Preparation of [AuCl(Ph$_2$PfcCONHCH$_2$CH$_2$OH-κP)] (**9**)

Ligand **3** (92 mg, 0.2 mmol) and [AuCl(tht)] (64 mg, 0.2 mmol) were mixed in dichloromethane (5 mL) and the resulting solution was stirred at room temperature for 1 h. Then, it was concentrated under vacuum and precipitated by addition of hexanes (5 mL). The suspension was cooled to −18 °C overnight before the precipitate was filtered off, washed with diethyl ether (2 × 5 mL) and dried under vacuum. A subsequent crystallization by slow diffusion of

hexanes into ethyl acetate solution of **9** afforded the gold(I) complex as orange crystals. Yield 113 mg (82%). ^{1}H NMR ($CDCl_3$): δ 3.11 (t, $^3J_{HH}$ = 5.4 Hz, 1H, OH), 3.63 (virtual q, J_{HH} = 5.0 Hz, 2H, CH_2O), 3.84 (virtual t, J_{HH} = 5.0 Hz, 2H, NHCH_2), 4.14 (virtual t, $J \approx 2$ Hz, 2H, fc), 4.27–4.28 (m, 2H, fc), 4.70–4.71 (m, 2H, fc), 4.93 (virtual t, $J \approx 2$ Hz, 2H, fc), 6.64 (t, $^3J_{HH}$ = 5.0 Hz, 1H, N*H*CH$_2$), 7.48–7.62 (m, 10H, PPh_2). ^{31}P{^{1}H} NMR ($CDCl_3$): δ 28.6 (s). IR (Nujol): ν_{NH} 3361 m, amide I 1624 s, amide II 1534 vs cm^{-1}. MS (ESI$^+$): *m*/*z* 712 ([M + Na]$^+$), 676 ([M − HCl + Na]$^+$), 654 ([M − Cl]$^+$). MS (ESI$^-$): *m*/*z* 689 ([M − H]$^-$). Anal. Calcd. for $C_{25}H_{24}PFeO_2NClAu$: C 43.53, H 3.51, N 2.03%. Found: C 43.24, H 3.51, N 1.91%.

4.5. Preparation of [AuCl(Ph$_2$PfcCONHCH(CH$_2$OH)$_2$-κP)] (**10**)

Complex **10** was prepared similarly to **9** starting from **4** (98 mg, 0.2 mmol) and [AuCl(tht)] (64 mg, 0.2 mmol), and was isolated as a yellow powder. Yield 130 mg (90%). ^{1}H NMR ($CDCl_3$): δ 3.30 (br t, $^3J_{HH}$ = 5.2 Hz, 2H, OH), 3.86–3.96 (m, 4H, CH_2O), 4.09–4.15 (m, 1H, NHC*H*), 4.16 (virtual t, $J \approx 2$ Hz, 2H, fc), 4.34–4.36 (m, 2H, fc), 4.69–4.71 (m, 2H, fc), 4.87 (virtual t, $J \approx 2$ Hz, 2H, fc), 6.67 (d, $^3J_{HH}$ = 7.0 Hz, 1H, N*H*CH), 7.44–7.59 (m, 10 H, PPh_2). ^{31}P{^{1}H} NMR ($CDCl_3$): δ 28.6 (s). IR (Nujol): ν_{NH} 3343 m, amide I 1633 s, amide II 1537 s cm^{-1}. MS (ESI$^+$): *m*/*z* 742 ([M + Na]$^+$), 706 ([M − HCl + Na]$^+$), 684 ([M − Cl]$^+$). MS (ESI−): *m*/*z* 718 ([M − H]$^-$). Anal. Calcd. for $C_{26}H_{26}PFeO_3NClAu$: C 43.39, H 3.64, N 1.95%. Found: C 43.16, H 3.58, N 1.78%.

4.6. Preparation of [AuCl(Ph$_2$PfcCONHC(CH$_2$OH)$_3$-κP)] (**11**)

Starting from **5** (104 mg, 0.2 mmol) and [AuCl(tht)] (64 mg, 0.2 mmol), the above procedure afforded **11** as a yellow powder. Yield 131 mg (87%). ^{1}H NMR ($CDCl_3$): δ 3.75 (d, $^3J_{HH}$ = 4.5 Hz, 6H, CH_2O), 4.00 (unresolved t, 3H, OH), 4.17 (virtual t, $J \approx 2$ Hz, 2H, fc), 4.36–4.38 (m, 2H, fc), 4.69–4.70 (m, 2H, fc), 4.78 (virtual t, $J \approx 2$ Hz, 2H, fc), 6.88 (s, 1H, N*H*C), 7.44–7.59 (m, 10 H, PPh_2). ^{31}P{^{1}H} NMR ($CDCl_3$): δ 28.5 (s). IR (Nujol): ν_{NH} 3373 s, amide I 1636 s, amide II 1525 s cm^{-1}. MS (ESI$^+$): *m*/*z* 772 ([M + Na]$^+$), 736 ([M − HCl + Na]$^+$), 714 ([M − Cl]$^+$). MS (ESI$^-$): *m*/*z* 748 ([M − H]$^-$). Anal. Calcd. for $C_{27}H_{28}PFeO_4NClAu$: C 43.25, H 3.76, N 1.87%. Found: C 43.79, H 3.72, N 1.77%.

4.7. Preparation of (HNEt$_3$)[AuCl(Ph$_2$PfcCONHCH$_2$SO$_3$-κP)] (**12**)

Complex **12** was obtained similarly from **6** (122 mg, 0.2 mmol) and [AuCl(tht)] (64 mg, 0.2 mmol) and isolated as a yellow powder. The precipitate obtained by filtration tends to retain solvents. The complex was therefore dissolved in a small amount of dichloromethane (3 mL), carefully evaporated to dryness at reduced pressure and dried under vacuum. Yield 155 mg (92%). ^{1}H NMR ($CDCl_3$): δ 1.34 (t, $^3J_{HH}$ = 7.3 Hz, 9H, CH_3 of Et_3NH^+), 3.16 (q, $^3J_{HH}$ = 7.3 Hz, 6H, CH_2 of Et_3NH^+), 4.38 (virtual t, $J \approx 2$ Hz, 2H, fc), 4.44–4.48 (m, 4H, fc and NHCH_2), 4.75 (virtual t, $J \approx 2$ Hz, 2H, fc), 4.83 (virtual q, $J \approx 2$ Hz, 2H, fc), 6.80 (br t, $^3J_{HH} \approx 6.3$ Hz, 1H, N*H*CH$_2$), 7.44–7.60 (m, 10 H, PPh_2). ^{31}P{^{1}H} NMR ($CDCl_3$): δ 28.7 (s). IR (Nujol): ν_{NH} 3281m, amide I 1648s, amide II 1537 s cm^{-1}. MS (ESI+): *m*/*z* 800 ([ClAu(Ph$_2$PfcCONHCH$_2$SO$_3$) + Na + K]$^+$), 784 ([ClAu(Ph$_2$PfcCONHCH$_2$SO$_3$) + 2Na]$^+$), 726 ([M − Cl + Na]$^+$). MS (ESI$^-$): *m*/*z* 738 ([ClAu(Ph$_2$PfcCONHCH$_2$SO$_3$)]$^-$). Anal. Calcd. for $C_{30}H_{37}PFeO_4N_2SAuCl$: C 42.85, H 4.44, N 3.33%. Found: C 41.89, H 4.46, N 3.14%.

4.8. X-ray crystallography

Crystal data for **7**: $C_{26}H_{24}AuClFeNO_3P$, M = 717.7, orange prism, 0.10 × 0.11 × 0.27 mm^3, monoclinic, space group $P2_1/c$ (no. 14), a = 19.2763(5), b = 9.8191(2), c = 13.5833(4) Å; β = 109.404(1)°; V = 2425.0(1) Å^3, Z = 4, D_{calc} = 1.97 g mL^{-1}.

Full-set diffraction data ($\pm h \pm k \pm l$) were recorded with an Apex 2 (Bruker) diffractometer equipped with Cryostream Cooler (Oxford Cryosystems) using graphite-monochromated Mo Kα radiation (λ = 0.71073 Å) at 150(2) K. The data were corrected for absorption (μ = 6.85 mm^{-1}) using a numerical method as incorporated in the diffractometer software. A total of 41,939 diffractions was recorded (θ_{max} = 27.5°, data completeness = 100%), from which 5562 were unique (R_{int} = 2.87%), and 5078 were observed according to the $I > 2\sigma(I)$ criterion.

The structure was solved by direct methods (SHELXS97 [27]) and refined by full-matrix least-squares routine based on F^2 (SHELXL97 [27]). The non-hydrogen atoms were refined with anisotropic displacement parameters. Hydrogens bonding to carbon atoms were included in their calculated positions and refined as riding atoms with U_{iso}(H) assigned to 1.2 or 1.5U_{eq}(C). The NH hydrogens were identified on a difference Fourier map and refined as riding atoms with U_{iso}(H) = 1.2U_{eq}(N). The refinement converged ($\Delta/\sigma \leq 0.002$, 308 parameters) to R = 1.66% for the observed, and R = 2.02%, wR = 3.52% for all diffractions. The final difference map displayed no peaks of chemical significance ($\Delta\rho_{max}$ = 1.20, $\Delta\rho_{min}$ = −0.56 e Å^{-3}).

Crystal data for **9**: $C_{25}H_{24}AuClFeNO_2P$, M = 689.7, orange prism (0.18 × 0.25 × 0.25 mm^3), triclinic, space group $P\bar{1}$ (no. 2), a = 10.6818(2), b = 12.6034(2), c = 19.7850(4) Å; α = 72.424(1)°, β = 89.3664(9)°, γ = 68.673(1)°; V = 2350.69(7) Å^3, Z = 4, D_{calc} = 1.95 g mL^{-1}.

The diffraction data were recorded similarly and were corrected for absorption (μ = 7.06 mm^{-1}) by an integration method included in the diffractometer software. A total of 45,773 diffractions was collected (θ_{max} = 27.5°, data completeness = 99.8%), from which 10,782 were unique (R_{int} = 5.51%), and 8121 were observed according to the $I > 2\sigma(I)$ criterion.

The refinement performed similarly to that of **7** converged ($\Delta/\sigma \leq 0.001$, 577 parameters) to R = 3.43% for the observed, and R = 5.53%, wR = 8.12% for all diffractions. The final difference map displayed no peaks of chemical significance; the largest residual electron density peaks were detected in vicinity of the Au atoms ($\Delta\rho_{max}$ = 1.41, $\Delta\rho_{min}$ = −2.34 e Å^{-3}).

4.9. Antiproliferative assays

Human A2780 and A2780cisR cells were obtained from the European Centre of Cell Cultures (ECACC, Salisbury, UK). All cell culture reagents were obtained from Gibco-BRL (Basel, Switzerland). Cells were grown in RPMI 1640 medium containing 10% fetal bovine serum (FBS) and antibiotics (100 IU/mL penicillin and 100 μg/mL streptomycin (Gibco)) and kept in a CO_2 incubator with 5% CO_2 and 100% relative humidity at 37 °C. Stock solutions of the complexes (in DMSO) were diluted in complete medium to the required concentration. DMSO at comparable concentrations did not show any effects on cell cytotoxicity.

For cytotoxicity screening, the cells were grown in 96-well cell culture plates (SPL Lifesciences) at a density of 20–25 × 10^3 cells per well. The culture medium was replaced with fresh medium containing the complexes at concentrations varying from 0 to 30 μM, with an exposure time of 72 h. Thereafter, cell survival was determined using the MTT test. A solution of 3-(4,5-dimethyl-2-thiazoyl)-2,5-diphenyltetrazolium bromide (MTT, Merck; 5 mg mL^{-1} in PBS; 20 μL per 200 μL of medium) was added to each well and incubation was continued for 2 h at 37 °C. Then the cell culture supernatants were removed, the cell layer was dissolved in DMSO, and absorbance at 590 nm was measured in a 96-well microplate reader (Spectramax M5e, Molecular Devices,

Sunnyvale, CA, USA) and compared to the values of control cells incubated in the absence of complexes. Experiments were conducted in triplicate wells and repeated at least twice.

Acknowledgments

The results reported in this paper were obtained with the support from the Ministry of Education, Youth and Sports of the Czech Republic (project no MSM0021620857) and partly also from the Czech Science Foundation (project no. 13-08890S).

Appendix A. Supplementary material

CCDC 943699 and 943700 contain the supplementary crystallographic data for this paper. These data can be obtained free of charge from The Cambridge Crystallographic Data Centre via www.ccdc.cam.ac.uk/data_request/cif.

References

[1] P. Štěpnička, Chem. Soc. Rev. 41 (2012) 4273.
[2] (a) J. Podlaha, P. Štěpnička, J. Ludvík, I. Císařová, Organometallics 15 (1996) 543; (b) P. Štěpnička, Eur. J. Inorg. Chem. (2005) 3787.
[3] J. Schulz, I. Císařová, P. Štěpnička, Organometallics 31 (2012) 729.
[4] J. Tauchman, I. Císařová, P. Štěpnička, Organometallics 28 (2009) 3288.
[5] (a) J. Tauchman, I. Císařová, P. Štěpnička, Eur. J. Org. Chem. (2010) 4276; (b) J. Tauchman, I. Císařová, P. Štěpnička, Dalton Trans. 40 (2011) 11748; (c) J. Tauchman, B. Therrien, G. Süss-Fink, P. Štěpnička, Organometallics 31 (2012) 3985.
[6] J. Schulz, I. Císařová, P. Štěpnička, J. Organomet. Chem. 694 (2009) 2519.
[7] J. Schulz, I. Císařová, P. Štěpnička, Eur. J. Inorg. Chem. (2012) 5000.
[8] A.A. Nazarov, P.J. Dyson, in: M. Peruzzini, L. Gonsalvi (Eds.), Catalysis by Metal Complexes: Phosphorus Compounds, vol. 37, 2011, pp. 445–461.
[9] C.F. Shaw, Chem. Rev. 99 (1999) 2589.
[10] G.F. Rush, P.F. Smith, G.D. Hoke, D.W. Alberts, R.M. Snyder, C.K. Mirabelli, Toxicol. Appl. Pharmacol. 90 (1987) 391.
[11] (a) C.K. Mirabelli, R.K. Johnson, D.T. Hill, L.F. Faucette, G.R. Girard, G.Y. Kuo, C.M. Sung, S.T. Crooke, J. Med. Chem. 29 (1986) 218; (b) C.K. Mirabelli, D.T. Hill, L.F. Faucette, F.L. McCabe, G.R. Girard, D.B. Bryan, B.M. Sutton, J.O. Bartus, S.T. Crooke, R.K. Johnson, J. Med. Chem. 30 (1987) 2181; (c) E.R.T. Tiekink, Crit. Rev. Oncol. Hematol. 42 (2002) 225.
[12] (a) N. Metzler-Nolte, M. Salmain, in: P. Štěpnička (Ed.), Ferrocenes: Ligands, Materials and Biomolecules, Wiley, Chichester, 2008, pp. 499–639 (chapter 13); (b) M.F.R. Fouda, M.M. Abd-Elzaher, R.A. Abdelsamaia, A.A. Labib, Appl. Organomet. Chem. 21 (2007) 613.
[13] (a) P. Köpf-Maier, H. Köpf, E.W. Neuse, J. Cancer Res. Clin. 108 (1984) 336; (b) L.V. Popova, V.N. Babin, Y.A. Belousov, Y.S. Nekrasov, A.E. Snegireva, N.P. Borodina, G.M. Shaposhnikova, O.B. Bychenko, P.M. Raevskii, Appl. Organomet. Chem. 7 (1993) 85.
[14] E. Hillard, A. Vessieres, F. Le Bideau, D. Plażuk, D. Spera, M. Huché, G. Jaouen, Chem. Med. Chem. 1 (2006) 551 (and references cited therein).
[15] W. Henderson, S.R. Alley, Inorg. Chim. Acta 322 (2001) 106.
[16] J. Schulz, A.K. Renfrew, I. Císařová, P.J. Dyson, P. Štěpnička, Appl. Organomet. Chem. 24 (2010) 392.
[17] J. Tauchman, G. Süss-Fink, P. Štěpnička, O. Zava, P.J. Dyson, J. Organomet. Chem. 723 (2013) 233.
[18] J. Kühnert, P. Ecorchard, H. Lang, Eur. J. Inorg. Chem. (2008) 5125.
[19] J.E. Aguado, S. Canales, M.C. Gimeno, P.G. Jones, A. Laguna, M.D. Villacampa, Dalton Trans. (2005) 3005.
[20] P. Štěpnička, M. Zábranský, I. Císařová, Chem. Open 1 (2012) 71.
[21] U. Siemeling, T. Klemann, C. Bruhn, J. Schulz, P. Štěpnička, Z. Anorg. Allg. Chem. 637 (2011) 1824.
[22] H. Schmidbaur, A. Schier, Chem. Soc. Rev. 41 (2012) 370 (and references cited therein).
[23] E. Vergara, E. Cerrada, C. Clavel, A. Casini, M. Laguna, Dalton Trans. 40 (2011) 10927.
[24] W.-H. Ang, A. Casini, G. Sava, P.J. Dyson, J. Organomet. Chem. 696 (2011) 989.
[25] A. De Luca, C.G. Hartinger, P.J. Dyson, M. Lo Bello, A. Casini, J. Inorg. Biochem. 119 (2013) 38.
[26] R. Uson, A. Laguna, M. Laguna, Inorg. Synth. 26 (1989) 85.
[27] G.M. Sheldrick, Acta Crystallogr. Sect. A, Fundam. Crystallogr. 64 (2008) 112.